analytical chemistry

pubs.acs.org/ac Article

Engineering a Rolling-Circle Strand Displacement Amplification Mediated Label-Free Ultrasensitive Electrochemical Biosensing Platform

Xiao-Long Zhang,[†] Yu-Han Liu,[†] Shu-Min Du, Yang Yin, Ling-Qi Kong, Yuan-Yuan Chang, Ya-Qin Chai, Zhao-Hui Li,* and Ruo Yuan*

Cite This: *Anal. Chem.* 2021, 93, 9568−9574 Read Online

ACCESS | Metrics & More | Article Recommendations | Supporting Information

ABSTRACT: In this work, an original rolling-circle strand displacement amplification (RC-SDA) was developed by introducing a circle DNA with two recognition domains as a template instead of the limited liner DNA template in traditional strand displacement amplification (SDA), which displayed much shorter reaction time down to 30 min and quite higher conversion efficiency of more than 1.77×10^8 compared with those of traditional strand displacement amplification (SDA) and could be applied to construct a label-free biosensor for ultrasensitive detection of an HIV DNA fragment. Once the target HIV DNA fragment interacts with the template circle DNA, the RC-SDA could be activated to dramatically output amounts of mimic target DNA with the assistance of the Phi29 DNA polymerase and Nb.BbvCI enzyme. In application, while the output products were captured by the DNA tetrahedral nanoprobe (DTNP) modified electrode, the electrochemical tag silver nanoclusters (AgNCs) on DTNP would be released from the electrode surface, accompanied with an obviously decreased electrochemical signal. This way, the developed signal-off biosensor was successfully applied to realize the rapid and ultrasensitive detection of target HIV DNA fragment with a detection limit down to 0.21 fM, which exploits the new generation of a universal strategy beyond the traditional ones for applications in biosensing assay, clinic diagnosis, and DNA nanobiotechnology.

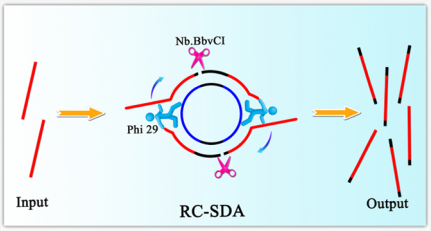

INTRODUCTION

Owing to the highly predictable base pairings, low cost, and excellent biocompatibility, synthetic nucleic acids have been widely applied in biotechnology research,[1] nanostructure construction,[2] signal amplification,[3] and so on.[4] Among these, amounts of nucleic acid signal amplifications with excellent designability and adequate performance were developed for achieving a more sensitive detection of various biomarker molecules.[5−7] However, most conventional methods like methylation-target polymerase chain reaction (PCR)[8] and radioactive labeling-based gel electrophoresis[9] suffered from complicated and time-consuming issues, which largely limit their application in resource-limited settings and for point-of-care (POC) analysis.[10] Alternatively, some isothermal amplifications of nucleic acids like strand displacement amplification (SDA)[11−13] and loop-mediated isothermal amplification (LAMP)[14,15] have been widely proposed in which simple condition, rapid, and efficient amplification is achieved. Nevertheless, the activity of the enzyme used in such liner amplification is obviously limited by the steric hindrance of single recognition domain and the restricted path of the enzyme reaction from the origin to the destination, which prevented the further exploration for advancing the rate and amplification efficiency of these strategies. In this respect, a rapid and highly efficient isothermal amplification that could maximize the reaction efficiency of enzyme is highly desirable.

Inspired by the typical rolling-circle amplification (RCA),[16,17] herein, an ingenious rolling-circle strand displacement amplification (RC-SDA) was developed by introducing a circle DNA strand as the template instead of the traditional limited liner DNA template, in which the dual recognition domain of target and unlimited amplification path without destination dramatically promote the reactivity of the enzyme, resulting in the high amplification efficiency and fast reaction speed. As a proof of concept, combining the Ag nanoclusters (AgNCs) synthesized in situ[18,19] with controllable performance as a strong electrochemical signal tag and the DNA tetrahedron nanostructure with high stability, strong rigidity, and outstanding lodging resistance[20,21] as a capture probe, the RC-SDA was successfully applied to construct an ultrasensitive biosensor for the detection of the HIV DNA fragment. The mechanism of the RC-SDA and biosensor construction was shown in Scheme 1. Firstly, the circle DNA template with two recognition domains was prepared with the T4 DNA ligase[22,23]

Received: April 20, 2021
Accepted: June 17, 2021
Published: July 1, 2021

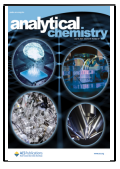

https://doi.org/10.1021/acs.analchem.1c01677
Anal. Chem. 2021, 93, 9568−9574

Scheme 1. (Part A) Synthesis Process of the Circle DNA Template; (Part B) Schematic Illustration of the Rolling-Circle Strand Displacement Amplification (RC-SDA); and (Part C) Illustration of the Biosensing Platform Construction Based on RC-SDA for HIV DNA Fragment Detection

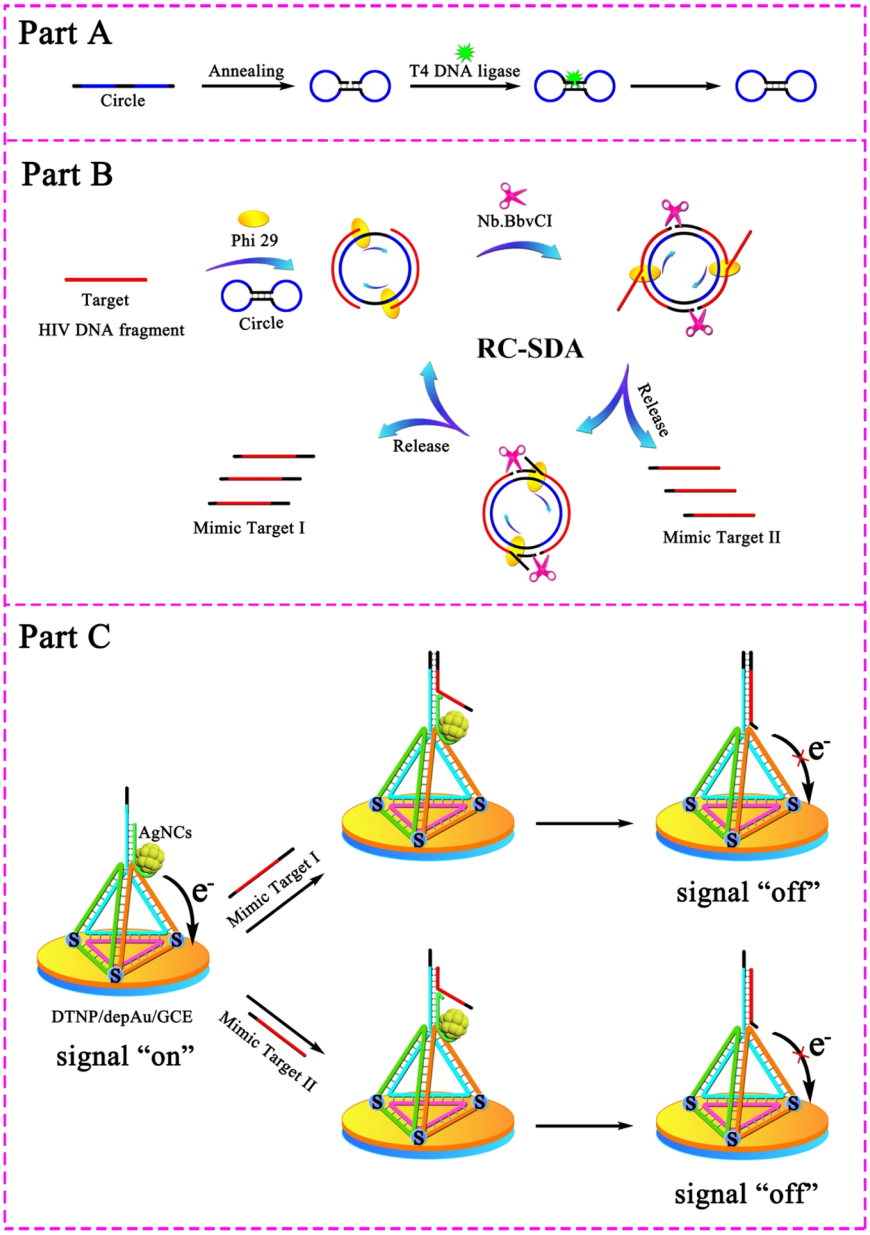

(Part A). Subsequently, once the target HIV DNA fragment is recognized by the circle DNA template, the RC-SDA will be triggered and amounts of mimic target DNA I and II could be outputted rapidly with the aid of the Phi29 DNA polymerase[24] and Nb.BbvCI enzyme[25] (Part B). Moreover, as displayed in Part C, the prepared DNA tetrahedral nanoprobe (DTNP) is immobilized on the electrode surface through a Au−S bond and the electrochemical signal tag AgNCs is then synthesized in situ on the overhang DNA strand Lock of DTNP, resulting in the obvious electrochemical signal response. While mimic target DNA I and II from RC-SDA are dropped onto the electrode modified DTNP, the overhang DNA Lock in DTNP will be displaced based on the toehold strand displacement reaction (TSDR),[26] accompanied with lots of released signal tag AgNCs from the electrode surface and resulting in the dramatically decreased electrochemical signal response. In this way, traces of the target HIV DNA fragment can induce amounts of electrochemical signal tag AgNCs released, achieving the conversion of signal "on" into signal "off" and the ultrasensitive detection of the HIV DNA fragment. Thus, this strategy provides a new insight to explore excellent nucleic acid signal amplification for further application of nucleic acid and biomarker detection in nascent stages of diseases.

EXPERIMENTAL SECTIONS

Preparation of the DNA Tetrahedron Nanoprobe. Equimolar quantities of five strands (A17, B17, C17, D17, and Lock) for the preparation of DTNP were mingled in a TM buffer (TCEP 1 mM, pH 8.0) with a concentration of 1 μM and heated to 95 °C subsequently for 10 min and cooled to 4 °C over 10 min. The prepared DTNPs were used in the subsequent experiments.

https://doi.org/10.1021/acs.analchem.1c01677
Anal. Chem. 2021, 93, 9568−9574

Assembly of the Elaborated Biosensor. First, the bare GCE (4 mm in diameter) was polished carefully with alumina slurry (0.3 and 0.05 μm) and treated by ultrasonic way with distilled water and ethanol. Subsequently, the fresh electrode was electrodeposited at −0.2 V for 30 s to coat a layer of gold particles (depAu) in $HAuCl_4$ aqueous solution (1%).

Next, the DTNP solution (10 μL, 1.0 μM) was added onto the surface of the modified electrode (depAu/GCE) and incubated overnight at room temperature. After being washed by the TM buffer to clear the DNA that adsorbed nonspecifically, the electrode was then rinsed by ethanol and distilled water for three times.

Preparation of the Ag Nanoclusters (AgNCs). To synthesize the Ag nanoclusters (AgNCs) in situ, the electrode modified DTNP containing AgNC template DNA strand (Lock) was rinsed by an HB buffer (10 mM Tris−HCl, 500 mM NaCl, and 1 mM $MgCl_2$, pH 7.4) and dried. Then, the $AgNO_3$ solution (10 μL, 100 μM) in a citrate buffer (20 mM, pH 7.0) was added onto the modified electrode surface (MCH/DTNP/depAu/GCE) for 20 min in the dark. Afterward, the freshly prepared $NaBH_4$ solution (2 μL, 500 μM) in the citrate buffer was carefully dropped onto the electrode surface above that covered with the $AgNO_3$ solution to reduce $AgNO_3$ to AgNCs[24] in situ on DNA Lock in DTNP immobilized on the electrode (room temperature, dark, 2 h). Lastly, the electrodes were rinsed by PBS (150 mM, pH 5.5) for subsequent electrochemical measurements.

Preparation of the Well-Designed Circular Template. The synthetic procedure of the circular template was outlined based on previous literature[27] with some modifications, as follows: First, 1 nM of the circle DNA template solution was dispersed in the Tris−HCl buffer (pH 7.4). Then, the solution was heated to 95 °C for 10 min and slowly cooled down to room temperature for 1 h to form the dual-hairpin nanostructure. After adding the 1× T4 DNA ligase reaction buffer and T4 DNA ligase (1 U/μL), the mixed solution was incubated at 16 °C for 12 h to conduct the intramolecular ligation. Lastly, the solution was treated with a thermal treatment (65 °C, 10 min) to terminate the reaction by inactivating the T4 DNA ligase, and the obtained products were stored at 4 °C for subsequent use.

Reaction of the Rolling-Circle Strand Displacement Amplification (RC-SDA). For feasibility investigation of RC-SDA, 1 nM HIV DNA fragment, 1 nM circle template, 500 μM dNTPs, 100 U/mL Nb.BbvCI, and 100 U/mL phi29 were mixed together and the mixture solution was placed at 37 °C in a constant-temperature incubator. Finally, the reaction solution was terminated by thermal treatment (65 °C, 10 min), and the obtained products were stored in a refrigerator (4 °C).

Polyacrylamide-Gel Electrophoresis (PAGE). After the DNA samples were mingled with the DNA-loading buffer (volume ratio 5:1), the different DNA-assembled products were analyzed by polyacrylamide-gel electrophoresis (PAGE) on a freshly prepared 16% polyacrylamide gel in 1× TBE buffer (30 mA, pH 8.0).

RESULTS AND DISCUSSION

Characterization of the RC-SDA and DTNP. Through the comparison of the biosensing platform based on the RC-SDA with different amounts of nicking sites in circle DNA, two nicking sites were fixed in the RC-SDA for the optimal performance (Supporting Information, pages S5 and S6, Figure S1). Under the optimal experimental conditions (Supporting Information, pages S6−S8, Figure S2), the self-assembly of RC-SDA and DTNP was characterized by PAGE. As displayed in Figure 1A, the bands in lanes 1 and 2 represent the target

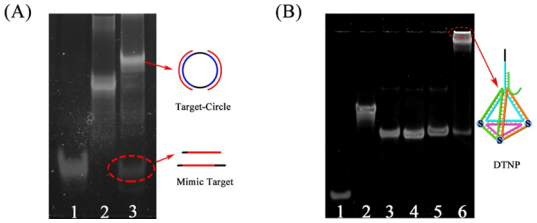

Figure 1. Nondenaturing PAGE characterization of (A) RC-SDA: lane 1, HIV DNA fragment (4 μM); lane 2, circle (2 μM); and lane 3, HIV DNA fragment (1 nM) and circle (2 μM) (with the aid of the Phi29 DNA polymerase and Nb.BbvCI enzyme) (PAGE 16%, 30 mA, 90 min); (B) DTNP: lane 1, lock-6c (2 μM); lane 2, A17 (2 μM); lane 3, B17 (2 μM); lane 4, C17 (2 μM); lane 5, D17 (2 μM); and lane 6, the mixture of A17 (2 μM), B17 (2 μM), C17 (2 μM), and D17 (2 μM) (PAGE 16%, 30 mA, 90 min).

HIV DNA fragment (4 μM) and circle DNA (2 μM), respectively. After the RC-SDA was triggered by a 1 nM target HIV DNA fragment, a band with slower migration corresponding to the complex target HIV DNA fragment−circle and a band with fast migration corresponding to mimic targets can be observed, illustrating the successful accomplishment of RC-SDA. Next, as exhibited in Figure 1B, the distinct bands in lanes 1−5 correspond to DNA Lock, A17, B17, C17, and D17 separately. After these five DNA strands were mixed to form DTNP, only one obvious band corresponding to DTNP could be noticed (lane 6) when compared with lanes 1−5, which verified that the DTNP was formed successfully. Moreover, we also adopted the atomic force microscope (AFM) to successfully characterize the size of DTNP (5.5 nm) and AgNCs (2.1 nm) (Supporting Information, pages S9 and S10, Figures S3 and S4).

Experimental Conversion Efficiency *N* of RC-SDA. To verify the extraordinary performance of the developed RC-SDA, we measured the experimental conversion efficiency *N* of it by the electrochemical biosensing platform. And the relationship of the current response of biosensing platform and the concentration of the quantified independent HIV DNA fragment (the sequence of mimic target DNA is almost the same as that of the HIV DNA fragment) was firstly carried out based on the SWV. As shown in Scheme 1, Part C, the biosensing platform was directly incubated with different concentrations of the HIV DNA fragment, which can be directly captured by DTNP modified on the electrode surface through DNA strand displacement based on TSDR and cause an obvious change of current response on the electrode surface. As the results show in Figure 2A, as the concentration of the HIV DNA fragment increased from 1 nM to 1.1 μM (1×10^{-9}−1.1×10^{-6} M), the SWV current response decreased and displayed a fine linear relationship with the concentration (Figure 2B). The corresponding regression equation was $I = 6.0219 - 5.2039c$ ($R = -0.9991$; I and c represented the SWV current response and concentration of the independent HIV DNA fragment (almost the same as the mimic target DNA as the output product), separately; the unit of c was μM). Subsequently, based on the relationship between the current response of the biosensing platform and the different concentrations of the input target after being amplified

https://doi.org/10.1021/acs.analchem.1c01677
Anal. Chem. 2021, 93, 9568−9574

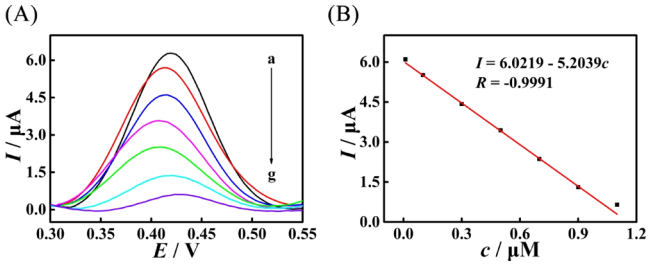

Figure 2. (A) SWV current responses of the biosensing platform to different concentrations of the HIV DNA fragment: (a) 1 nM, (b) 0.1 μM, (c) 0.3 μM, (d) 0.5 μM, (e) 0.7 μM, (f) 0.9 μM, and (g) 1.1 μM. (B) The calibration plot for the SWV peak current *vs* *c* (*c* represents the HIV DNA fragment concentration).

through RC-SDA (Figure 2), the accurate experimental conversion efficiency *N* of RC-SDA was calculated, with a wide range from 9.5×10^1 to 1.77×10^8 (the ratio of the output product concentration and input target concentration, Table S2).

Comparison of the RC-SDA with Traditional SDA. To verify that the RC-SDA (Figure 3A, a) achieves the

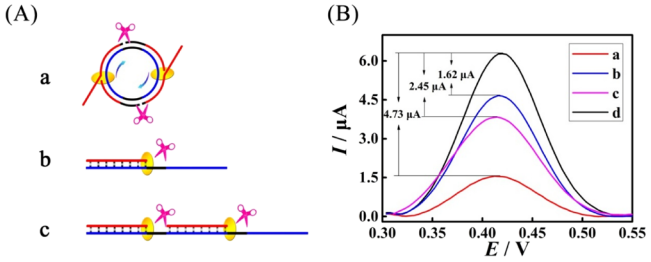

Figure 3. (A) Schematic illustration of (a) RC-SDA, (b) traditional SDA, and (c) SDA with two work sites. (B) Comparison of the SWV responses of (a) RC-SDA, (b) traditional SDA, (c) SDA with two sites, and (d) prepared biosensors under optimal conditions.

dramatically improved efficiency compared with the traditional SDA (Figure 3A, b and c), we compared the current response of the prepared biosensor to them with the same target HIV DNA fragment input. As exhibited in Figure 3B, when compared with the initial signal of the prepared biosensor (curve d), the corresponding current response change with the RC-SDA (4.73 μA, curve a) was almost three times higher than that with the SDA-1 ("1" means one recognition domain) (1.62 μA, curve b) and two times higher than that with SDA-2 ("2" means two recognition domains) (2.45 μA, curve c). Moreover, in contrast, the conversion efficiency (*N*) of RC-SDA (9.5×10^1–1.77×10^8) is quite higher than that of traditional SDA-1 (3.6×10^1–1.2×10^4) and SDA-2 (5.4×10^1–4.2×10^5) (Supporting Information, pages S11 and S12, Tables S2 and S3, and Figure S5), respectively. Otherwise, we compared the performance of RC-SDA with that of other typical isothermal amplification methods. As shown in Table 1, the RC-SDA displayed the least reaction time and excellent conversion efficiency even under low temperature. These results above illustrated that the proposed RC-SDA successfully addressed the challenges of these traditional nucleic acid amplifications: long reaction time and low efficiency.

The Feasibility of the Proposed Biosensing Platform for the HIV DNA Fragment Detection. To further prove that the developed RC-SDA could be applied as biosensing

Table 1. Comparison of the Original RC-SDA with Other Amplification Methods

method	temperature (°C)	reaction time (h)	efficiency	ref
HDA	37–65	0.5–2	10^7	28, 29
E-SDA	37	2	10^7	11, 30
MDA	30–37	8	10^6	31, 32
PG-RCA	60	1–3	~60 copies	33, 34
RC-SDA	37	0.5	9.50×10^1–1.77×10^8	this work

platform construction for HIV DNA fragment detection, the SWV was employed to compare the response of the biosensor under different conditions. As displayed in Figure 4, the

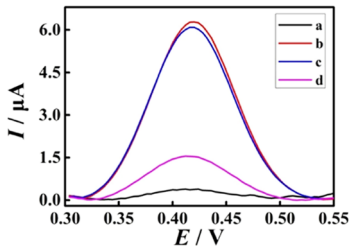

Figure 4. Comparison of the SWV responses of the prepared biosensor (a) without AgNC template DNA on the DTNP, (b) with AgNC template DNA on the DTNP, (c) incubated with independent HIV DNA fragment, and (d) incubated with the resultants after the HIV DNA fragment (1 nM) was introduced in RC-SDA.

prepared biosensing platform without AgNC template DNA (Lock) on the DTNP showed a negligible current response (curve a); however, while the AgNC template DNA existed, the current response of the biosensing platform showed an obvious value (curve b), illustrating that the AgNCs could only be largely synthesized in the presence of template DNA. After the independent HIV DNA fragment was incubated on the biosensor, the current response decreased slightly (curve c). Impressively, while the same HIV DNA fragment was amplified by the RC-SDA, the current response of the biosensor to it decreased dramatically (curve d), which indicated that the RC-SDA could be well applied into developing an ultrasensitive biosensor for HIV DNA fragment detection.

Performance of the Biosensor Based on RC-SDA. After the construction of the biosensing platform based on RC-SDA was successfully characterized by the CV and EIS (Supporting Information, page S13 and S14, Figure S6), a series of different concentration of HIV DNA fragment was used to study the detection performance of the established biosensing platform under the optimal conditions. As shown in Figure 5A, the SWV current response decreased gradually with the increased concentration of target from 0.1 fM to 10 nM and exhibited a well linear relationship with the logarithm of the HIV DNA fragment concentration. And as shown in Figure 5B, the corresponding regression equation is presented as $I = -0.6804 \lg c - 4.5849$ (I is the peak current value, and c is the concentration of the target HIV DNA fragment) with a correlation-coefficient value (R) of −0.9985. Impressively, when compared with other analytical methods, as illustrated in Table 2, the developed biosensing platform displayed a remarkably wider linear range and a quite lower detection limit (Supporting Information, page S14), which could be

https://doi.org/10.1021/acs.analchem.1c01677
Anal. Chem. 2021, 93, 9568–9574

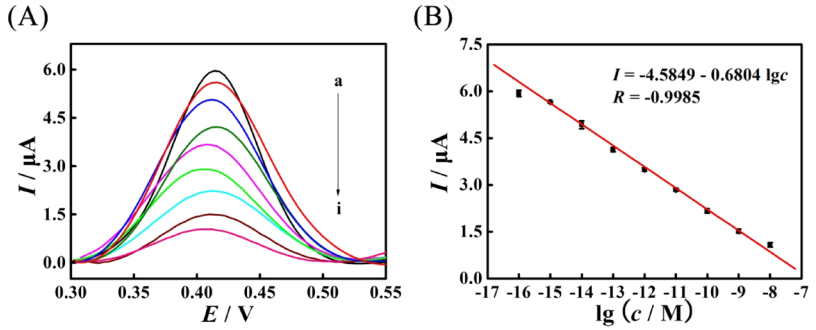

Figure 5. (A) SWV current responses of the biosensors to different concentrations of the target HIV DNA fragment: (a) 0.1 fM, (b) 1 fM, (c) 10 fM, (d) 100 fM, (e) 1 pM, (f) 10 pM, (g) 100 pM, (h) 1 nM, and (i) 10 nM. (B) Corresponding calibration plot for the SWV peak current *vs* lg c.

Table 2. Comparison of the Biosensor Developed by RC-SDA with Other Nucleic Acid Detection Methods

analytical methods	linear range	detection limit	ref
photoelectrochemical	1 fM−10 pM	0.5 fM	35
fluorescence	1pM−10 nM	0.35 pM	36
electroluminescence	0.05 pM−50 nM	39.81 fM	37
electrochemical	10 fM−20 nM	10 fM	38
electrochemical	100 fM−10 nM	150 fM	39
electrochemical	0.1 fM−1 nM	0.21 fM	this work

ascribed to the synergistic effect between the outstanding amplification efficiency of RC-SDA and the attractive capture efficiency of the DTNP.

Reproducibility, Selectivity, and Stability of the Biosensor. To further study the performance of this proposed biosensor comprehensively, the reproducibility, selectivity, and stability of the sensing platform that was prepared based on DTNP and evolved RC-SDA were validated. To confirm the reproducibility of the sensing platform, the necessary index for a real biomarker detection, four of the prepared biosensors with a 100 pM target HIV DNA fragment were studied under the same determination condition. As displayed in Figure 6A, a relative standard deviation (RSD) of 2.1% is achieved. Moreover, a set of electrodes with same HIV DNA fragment (100 pM) has been detected after 10 days, and the RSD is 0.86%. The remarkable results indicate that the combination of the evolved RC-SDA and DTNP for biomarker detection presented a desirable reproducibility.

To assess the selectivity of this biosensor, four interference agents including DNA-1, DNA-2, and DNA-3 were evaluated under the same experimental condition. As displayed in Figure 6B, the obvious current response of the electrode could be observed only with the presence of the HIV DNA fragment (100 pM). Oppositely, the current responses were negligible even with the interference agents including interferents DNA-1 (10 nM), DNA-2 (10 nM), and DNA-3 (10 nM). Besides, the mixed analytical solution containing 100 pM of the target HIV DNA fragment was also analyzed with the sensing system, exhibiting an obvious electrochemical signal as expected. The results above demonstrated the high selectivity of the biosensor based on the evolved RC-SDA and DTNP.

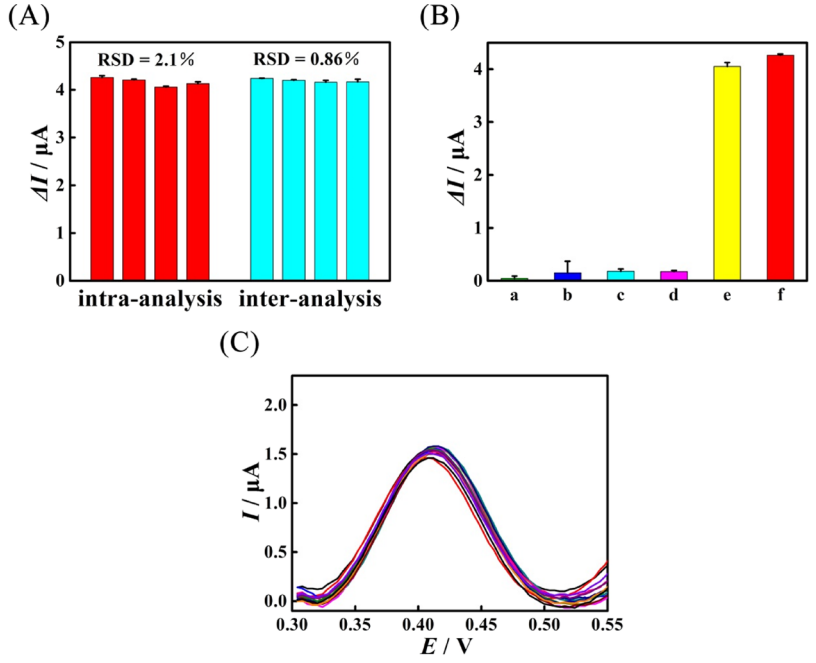

Figure 6. (A) The reproducibility (100 pM HIV DNA) of the biosensing platform. (B) The selectivity of the electrochemical biosensor: (a) blank sample, (b) DNA-1 (10 nM), (c) DNA-2 (10 nM), (d) DNA-3 (10 nM), (e) HIV DNA fragment (100 pM), and (f) mixed sample. (C) The stability of the elaborated biosensor (1 nM HIV DNA fragment).

https://doi.org/10.1021/acs.analchem.1c01677
Anal. Chem. 2021, 93, 9568−9574

The stability, which was critical to its practical application especially in a complicated biomedical environment, was evaluated by successive scans of the sensing platform with detection of a 1 nM target HIV DNA fragment for 15 times. As displayed in Figure 6C, when compared with the initial value of current response, the SWV current value only changed from 92.8 to 106.0% with the RSD = 3.95%, indicating a desirable stability of our biosensing surface.

Practical Application of the Developed Biosensor Based on the RC-SDA. To assess the effectiveness of this RC-SDA mediated electrochemical biosensor in practical applications, recovery experiments were performed using human serum. First, no HIV DNA fragment was found in tap water. Then, the serum samples spiked with an HIV DNA fragment at four different concentrations of 0.001, 0.01, 0.1, and 1 nM were tested, obtaining satisfactory recoveries in the range of 99.56 to 111.4% listed in Table 3. Thus, these testing results illustrated the potential application of this biosensor in real samples containing an HIV DNA fragment (the experimental ethics of human serum were supplied in Supporting Information, pages S14 and S15).

Table 3. Recovery Experiments of the HIV DNA Fragment in Serum

sample	added HIV DNA fragment (nM)	found HIV DNA fragment (nM)	recovery (%)	relative standard deviation, RSD (%)
1	0.001	0.001114	111.4	0.13
2	0.01	0.01072	107.2	3.61
3	0.1	0.1031	103.1	1.08
4	1	0.9956	99.56	4.54

CONCLUSIONS

In summary, unlike the traditional strand displacement amplification (SDA), the rolling-circle strand displacement amplification (RC-SDA) we propose realizes the pretty high conversion efficiency by introducing a circle DNA with two target recognition domains as template, which dramatically improve the reaction rate and conversion efficiency. Benefiting from this advantage, the RC-SDA is successfully applied to construct a biosensor for achieving the rapid and ultrasensitive detection of an HIV DNA fragment, which carves out a brand-new way to design a potential strategy for the biosensing assay and clinical diagnosis. Otherwise, the RC-SDA also proposes a creative insight to explore the inherent property of nucleic acid amplification for advancing its superiority and applicability in diagnostic applications, nanobiotechnology, and so on.

ASSOCIATED CONTENT

Supporting Information

The Supporting Information is available free of charge at https://pubs.acs.org/doi/10.1021/acs.analchem.1c01677.

Experimental sections; comparison of the RC-SDA with different amounts of nicking sites in circle DNA; exploration of different experimental conditions; electron microscope characterization of the DTNP and the AgNCs; experimental conversion efficiency N of RC-SDA with different concentrations of target by electrochemistry; experimental conversion efficiency N of SDA-1 and SDA-2 with different concentrations of target HIV DNA fragment by electrochemistry; electrochemical characterization of the biosensing platform; limit of detection calculation for the DNA biosensing; experimental ethics of human serum; and references (PDF)

AUTHOR INFORMATION

Corresponding Authors

Zhao-Hui Li − *Henan Joint International Research Laboratory of Green Construction of Functional Molecules and Their Bioanalytical Applications, College of Chemistry, Zhengzhou University, Zhengzhou 450001, P.R. China;* orcid.org/0000-0003-3946-0656; Email: zhaohui.li@zzu.edu.cn

Ruo Yuan − *Key Laboratory of Luminescence Analysis and Molecular Sensing (Southwest University), Ministry of Education, College of Chemistry and Chemical Engineering, Southwest University, Chongqing 400715, P.R. China;* orcid.org/0000-0003-3664-6236; Phone: +86 2368252277; Email: yuanruo@swu.edu.cn; Fax: +86 2368253172

Authors

Xiao-Long Zhang − *Key Laboratory of Luminescence Analysis and Molecular Sensing (Southwest University), Ministry of Education, College of Chemistry and Chemical Engineering, Southwest University, Chongqing 400715, P.R. China*

Yu-Han Liu − *Key Laboratory of Luminescence Analysis and Molecular Sensing (Southwest University), Ministry of Education, College of Chemistry and Chemical Engineering, Southwest University, Chongqing 400715, P.R. China*

Shu-Min Du − *Key Laboratory of Luminescence Analysis and Molecular Sensing (Southwest University), Ministry of Education, College of Chemistry and Chemical Engineering, Southwest University, Chongqing 400715, P.R. China*

Yang Yin − *Key Laboratory of Luminescence Analysis and Molecular Sensing (Southwest University), Ministry of Education, College of Chemistry and Chemical Engineering, Southwest University, Chongqing 400715, P.R. China*

Ling-Qi Kong − *Key Laboratory of Luminescence Analysis and Molecular Sensing (Southwest University), Ministry of Education, College of Chemistry and Chemical Engineering, Southwest University, Chongqing 400715, P.R. China*

Yuan-Yuan Chang − *Key Laboratory of Luminescence Analysis and Molecular Sensing (Southwest University), Ministry of Education, College of Chemistry and Chemical Engineering, Southwest University, Chongqing 400715, P.R. China*

Ya-Qin Chai − *Key Laboratory of Luminescence Analysis and Molecular Sensing (Southwest University), Ministry of Education, College of Chemistry and Chemical Engineering, Southwest University, Chongqing 400715, P.R. China;* orcid.org/0000-0003-4392-9592

Complete contact information is available at: https://pubs.acs.org/10.1021/acs.analchem.1c01677

Author Contributions

†X.-L. Zhang and Y.-H. Liu contributed equally.

Notes

The authors declare no competing financial interest.

ACKNOWLEDGMENTS

This paper was financially supported by the National Natural Science Foundation of China (21775124 and 21974108), China Postdoctoral Science Foundation (2019 M663417 and

2020 T130544), and the Fundamental Research Funds for the Central Universities (XDJK2019TJ002), China.

REFERENCES

(1) Thubagere, A. J.; Li, W.; Johnson, R. F.; Chen, Z.; Doroudi, S.; Lee, Y. L.; Izatt, G.; Wittman, S.; Srinivas, N.; Woods, D.; Winfree, E.; Qian, L. *Science* **2017**, *357*, No. eaan6558.
(2) Hao, Y.; Li, Y.; Song, L.; Deng, Z. *J. Am. Chem. Soc.* **2021**, *143*, 3065−3069.
(3) Ding, X.; Yin, K.; Li, Z.; Lalla, R. V.; Ballesteros, E.; Sfeir, M. M.; Liu, C. *Nat. Commun.* **2020**, *11*, 4711.
(4) Qing, Z.; Xu, J.; Hu, J.; Zheng, J.; He, L.; Zou, Z.; Yang, S.; Tan, W.; Yang, R. *Angew. Chem., Int. Ed.* **2019**, *58*, 11574−11585.
(5) Gines, G.; Menezes, R.; Nara, K.; Kirstetter, A. S.; Taly, V.; Rondelez, Y. *Sci. Adv.* **2020**, *6*, No. eaay5952.
(6) Oishi, M.; Saito, K. *ACS Nano* **2020**, *14*, 3477−3489.
(7) Zhou, Z.; Brennan, J. D.; Li, Y. *Angew. Chem., Int. Ed.* **2020**, *59*, 10401−10405.
(8) Zhang, Y.; Li, Q.; Guo, L.; Huang, Q.; Shi, J.; Yang, Y.; Liu, D.; Fan, C. *Am. Ethnol.* **2016**, *128*, 12638−12642.
(9) Zhang, D. Y.; Chen, S. X.; Yin, P. *Nat. Chem.* **2012**, *4*, 208−214.
(10) Dai, Y.; Wu, Y.; Liu, G.; Gooding, J. J. *Angew. Chem., Int. Ed.* **2020**, *59*, 20754−20766.
(11) Walker, G. T.; Fraiser, M. S.; Schram, J. L.; Little, M. C.; Nadeau, J. G.; Malinowski, D. P. *Nucleic Acids Res.* **1992**, *20*, 1691−1696.
(12) Koc, K. N.; Stodola, J. L.; Burgers, P. M.; Galletto, R. *Nucleic Acids Res.* **2015**, *43*, 4179−4190.
(13) Zhou, W.; Hu, L.; Ying, L.; Zhao, Z.; Chu, P.; Yu, X.-F. *Nat. Commun.* **2018**, *9*, 5012.
(14) Notomi, T.; Okayama, H.; Masubuchi, H.; Yonekawa, T.; Watanabe, K.; Amino, N.; Hase, T. *Nucleic Acids Res.* **2000**, *28*, e63.
(15) Tang, Z.; Choi, G.; Nouri, R.; Guan, W. *Nano Lett.* **2019**, *19*, 7927−7934.
(16) Hamblin, G. D.; Carneiro, K. M. M.; Fakhoury, J. F.; Bujold, K. E.; Sleiman, H. F. *J. Am. Chem. Soc.* **2012**, *134*, 2888−2891.
(17) Ali, M. M.; Li, F.; Zhang, Z.; Zhang, K.; Kang, D.-K.; Ankrum, J. A.; Le, X. C.; Zhao, W. *Chem. Soc. Rev.* **2014**, *43*, 3324−3341.
(18) Petty, J. T.; Zheng, J.; Hud, N. V.; Dickson, R. M. *J. Am. Chem. Soc.* **2004**, *126*, 5207−5212.
(19) Yang, C.; Shi, K.; Dou, B.; Xiang, Y.; Chai, Y.; Yuan, R. *ACS Appl. Mater. Interfaces* **2015**, *7*, 1188−1193.
(20) Pei, H.; Lu, N.; Wen, Y.; Song, S.; Liu, Y.; Yan, H.; Fan, C. *Adv. Mater.* **2010**, *22*, 4754−4758.
(21) Li, C.; Hu, X.; Lu, J.; Mao, X.; Xiang, Y.; Shu, Y.; Li, G. *Chem. Sci.* **2018**, *9*, 979−984.
(22) Kuhn, H.; Demidov, V. V.; Frank-Kamenetskii, M. D. *Nucleic Acids Res.* **2002**, *30*, 574−580.
(23) Kuhn, H.; Frank-Kamenetskii, M. D. *FEBS J.* **2005**, *272*, 5991−6000.
(24) Krzywkowski, T.; Kühnemund, M.; Wu, D.; Nilsson, M. *Nucleic Acids Res.* **2018**, *46*, 3625−3632.
(25) Zhang, Z.; Balogh, D.; Wang, F.; Sung, S. Y.; Nechushtai, R.; Willner, I. *ACS Nano* **2013**, *7*, 8455−8468.
(26) Zhang, D. Y.; Seelig, G. *Nat. Chem.* **2011**, *3*, 103−113.
(27) Chen, A.; Ma, S.; Zhuo, Y.; Chai, Y.; Yuan, R. *Anal. Chem.* **2016**, *88*, 3203−3210.
(28) Vincent, M.; Xu, Y.; Kong, H. *EMBO Rep.* **2004**, *5*, 795−800.
(29) Cao, A.; Zhang, C.-y. *Anal. Chem.* **2013**, *85*, 2543−2547.
(30) Shi, C.; Liu, Q.; Ma, C.; Zhong, W. *Anal. Chem.* **2014**, *86*, 336−339.
(31) Dean, F. B.; Hosono, S.; Fang, L.; Wu, X.; Faruqi, A. F.; Bray-Ward, P.; Sun, Z.; Zong, Q.; Du, Y.; Du, J.; Driscoll, M.; Song, W.; Kingsmore, S. F.; Egholm, M.; Lasken, R. S. *Proc. Natl. Acad. Sci.* **2002**, *99*, 5261−5266.
(32) Henke, W.; Herdel, K.; Jung, K.; Schnorr, D.; Loening, S. A. *Nucleic Acids Res.* **1997**, *25*, 3957−3958.
(33) Murakami, T.; Sumaoka, J.; Komiyama, M. *Nucleic Acids Res.* **2009**, *37*, e19.
(34) Murakami, T.; Sumaoka, J.; Komiyama, M. *Nucleic Acids Res.* **2012**, *40*, e22.
(35) Zhang, N.; Shi, X.-M.; Guo, H.-Q.; Zhao, X.-Z.; Zhao, W.-W.; Xu, J.-J.; Chen, H.-Y. *Anal. Chem.* **2018**, *90*, 11892−11898.
(36) Yang, Z.; Peng, X.; Yang, P.; Zhuo, Y.; Chai, Y.-Q.; Liang, W.; Yuan, R. *Chem. Sci.* **2020**, *11*, 8482−8488.
(37) Wu, Z.; Luo, F.; Wen, W.; Zhang, X.; Wang, S. *Anal. Chem.* **2019**, *91*, 12238−12245.
(38) Mensah, K.; Cissé, I.; Pierret, A.; Rosticher, M.; Palomo, J.; Morfin, P.; Plaçais, B.; Bockelmann, U. *Adv. Healthcare Mater.* **2020**, *9*, 2000260.
(39) Gao, X.; Wang, X.; Li, Y.; He, J.; Yu, H.-Z. *Anal. Chem.* **2018**, *90*, 8147−8153.

https://doi.org/10.1021/acs.analchem.1c01677
Anal. Chem. 2021, 93, 9568−9574